



Detailed investigation of flameless oxidation of pulverized coal at pilot-scale (230 kW_{th})



M. Weidmann ^{a,*}, V. Verbaere ^b, G. Boutin ^c, D. Honoré ^c, S. Grathwohl ^a, G. Goddard ^c, C. Gobin ^c, H. Dieter ^a, R. Kneer ^b, G. Scheffknecht ^a

^a Institute of Combustion and Power Plant Technology, University of Stuttgart, Pfaffenwaldring 23, 70176 Stuttgart, Germany

^b Institute of Heat and Mass Transfer, RWTH Aachen University, Eifelschornsteinstrasse 18, 52056 Aachen, Germany

^c CNRS, INSA de Rouen, Université de Rouen, 685 avenue de l'Université – BP 08, 76801 Saint Etienne du Rouvray, France

HIGHLIGHTS

- Related measurements of gas concentration, gas temperature and velocity of pulverized coal flameless oxidation.
- Identification of reaction zone topology by OH* chemiluminescence.
- Characterization of the formation and consumption of nitrogenous compounds by FTIR.
- Investigation of the use of CO₂ as coal carrier gas.

ARTICLE INFO

Article history:

Received 30 August 2013

Accepted 19 January 2014

Available online 27 January 2014

Keywords:

Flameless combustion

Pulverized coal

NO_x

ABSTRACT

Within this paper the detailed investigation of flameless oxidation (FLOX[®]) at the pilot-scale test facility at University of Stuttgart is presented. The experimental boundary conditions of two FLOX cases are given. Subsequently, the results obtained with OH* chemiluminescence imaging, velocity measurements and in-flame measurements of gas temperature and gas concentrations are described and interrelated. These clearly show the major features of FLOX e.g. delayed ignition, low reaction intensity as well as homogeneous temperature and radiation profiles. The root causes involved in the formation and reduction of nitric oxides are pointed out, e.g. the NO_x precursors and the oxygen concentrations. Special focus is drawn on the influence of the coal carrier gases air or CO₂.

© 2014 Elsevier Ltd. All rights reserved.

1. Introduction

Since the 1970s, the abatement of nitric oxide emissions from anthropogenic sources, such as combustion processes, has been an issue. Nitrogen monoxide (NO) and nitrogen dioxide (NO₂), grouped under the label NO_x, as well as nitrous oxide (N₂O) are known to harm the environment: one effect is the conversion to nitric acid (HNO₃) after contact with water in the Earth's atmosphere, followed by a deposition and acidification of the soil. Secondly the ozone layer within the stratosphere is affected due to the catalytic effect of nitrogen oxides resulting in a reformation of

ozone to oxygen. Finally, the N₂O contributes to the global warming due to its high absorptivity and its high lifetime within the stratosphere. Thus, over the last decades measures have been developed and established to reduce NO_x emissions from combustion processes. Primary measures, such as low NO_x burners or air staging, can directly affect the combustion process and are therefore widely used. However, secondary measures, i.e. post-combustion measures, such as selective catalytic reduction (SCR) are still necessary to comply with environmental restrictions. These are still accompanied by high operational costs. In the early 1990s, flameless oxidation (FLOX[®])¹ became a research topic in the field of NO_x abatement from combustion [1]. This technology first proved its NO_x-reduction potential for gaseous fuels, resulting in a reduced thermal N-conversion for high air preheating temperatures. Soon, the focus was directed towards other fuels, such as pulverized coals

Abbreviations: CFD, Computational Fluid Dynamics; FLOX, flameless oxidation; FTIR, Fourier transform infra-red; HiTAC, high temperature air combustion; LDV, Laser-Doppler-Velocimetry; MILD, moderate and intensive low-oxygen dilution; NDIR, non-dispersive infra-red; SCR, selective catalytic reduction.

* Corresponding author. Pfaffenwaldring 23, 70569 Stuttgart, Germany. Tel.: +49 711 685 67806.

E-mail address: max.weidmann@ifk.uni-stuttgart.de (M. Weidmann).

¹ FLOX[®] is a registered trademark of WS Wärme Prozess Technik GmbH, Renningen, Germany.

containing fuel-bound nitrogen. This was investigated by different researchers under the name of “High Temperature Air Combustion” (HiTAC) (see [2] and [3]) and “Moderate and Intensive Low-Oxygen Dilution” (MILD) [4]. These approaches showed a strong NO_x-reduction potential; however, additional measures like high-temperature air preheating, reactants preheating or combustion air dilution by flue gas recirculation were necessary.

2. Theory

The NO_x emissions from combustion processes originate from three sources: (i) prompt NO which is formed by the attack of hydrocarbon radicals on molecular nitrogen [5], (ii) thermal NO which implies the conversion of atmospheric nitrogen at high temperatures [6] and (iii) fuel NO which originates from the conversion of fuel-inherent nitrogen. According to several authors ([7] and [8]), prompt NO only contributes marginally to NO_x emissions in connection with coal-fired furnaces, therefore it is not further considered. By contrast the abatement of thermal NO and fuel NO formation considerably lowers NO_x emissions. The thermal NO path is strongly temperature dependent and is known as Zeldovich mechanism [6]. In conventional-fired furnaces, the meeting of high oxygen concentration with fuel results in a flame front characterized by high temperatures above 1300 °C. Consequently, high NO formation rates are achieved. By applying the FLOX technology, a stabilised flame front does not develop, leading to much lower and more homogeneous furnace temperatures. Thus, the thermal NO_x contribution can be reduced by 50% [9]. The third NO_x source in combustion processes originates from nitrogen bound in the combusted fuel. This so-called fuel N is converted via numerous paths during volatile combustion and char burnout [10]. The conversion depends less on the temperature than rather on the atmosphere composition: fuel-rich conditions promote the reduction of fuel-NO as it was identified during several experimental investigations conducted at bench-scale (20 kW_{th}) in the course of previous FLOX projects at IFK, University of Stuttgart [9]. Summarizing, the thermal NO_x formation can be diminished by the FLOX technology as the result of a lower temperature level and a more homogeneous temperature distribution. To this end, the oxygen availability is reduced within the pyrolysis and oxidation zones mitigating the combustion intensity. The incoming combustion air thereby entrains the surrounding flue gas and ensures an oxygen-lean atmosphere when combustion air and fuel mix together. Further NO_x reduction mechanisms such as the reburning by volatiles are promoted by adequate temperatures in the burner vicinity: the recirculated flue gas heats up the incoming coal jet and thus leads to a fast devolatilization. As a result, reburning and catalytic char reactions occur and NO_x emissions are reduced.

3. Experimental

The experiments reported in this paper were conducted at the 500 kW_{th} test rig at University of Stuttgart. It is a down-fired pulverized fuel furnace of cylindrical shape. Its axis is vertical to minimize asymmetry due to natural convection and biased ash particle deposition. The test rig is made up of six water-cooled segments with a total length of 7000 mm and an inner diameter of 750 mm. Several ports located all around the furnace allow in-flame measurements of gas composition, gas temperature and ash sampling in vertical and horizontal directions by means of specially designed probes. A detailed description of the facility can be found in Ristic [9].

The installed burner features a central annulus delivering coal and carrier gas. The combustion air is supplied through two nozzles symmetrically arranged. A sketch of the burner is shown in Fig. 1.

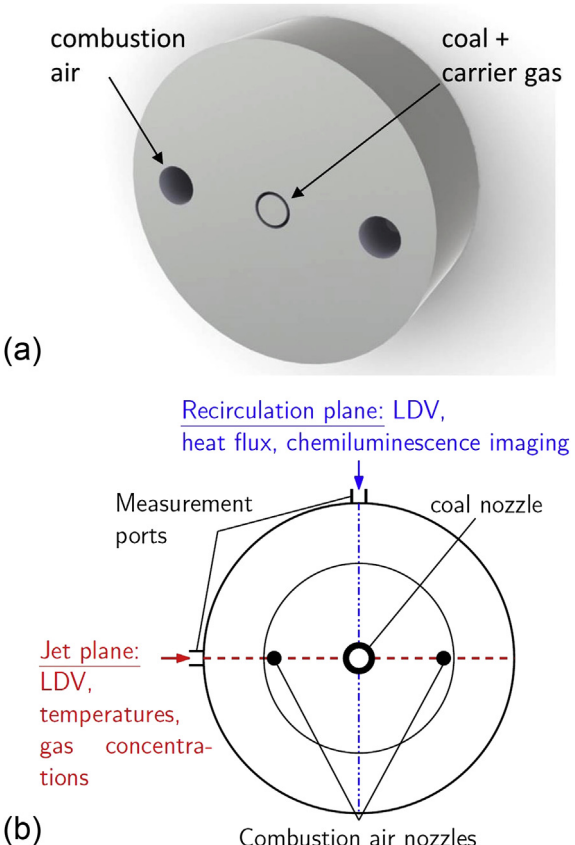


Fig. 1. (a) Applied burner and (b) measurement planes in the presented FLOX experiment.

The fuel burned in the experiments is the high-volatile sub-bituminous Columbian coal “Calentur”. Table 1 contains its proximate and ultimate data. In general terms, Calentur coal exhibits very similar properties to “El Cerrejón” coal, as well of Columbian origin and widely used in the German power industry. The Calentur coal is characterized by (i) a medium nitrogen content which prevents an excessive fuel NO_x formation and (ii) a high volatile content, beneficial to reduction reactions. The particle size distribution is given by a Rosin-Rammler spread parameter of 3.8 and a mean diameter of 80.5 µm.

A measurement grid is elaborated with a radial resolution of 25 mm in the near burner region and 100 mm in the outer region. In downstream direction, the resolution of the measurement grid is pre-set by the ports available: these are staggered 170 mm apart. This grid is applied to all conducted in-flame measurements in the jet plane and the recirculation plane. These planes are shown in Fig. 1b. The experimental investigation includes in-flame

Table 1
Proximate and ultimate analysis of Calentur coal.

Calentur	Basis	(wt-%)
Moisture	Raw	11.70
Ash	Dry	11.03
Volatiles	Dry ash free	42.28
Fixed C	Dry ash free	57.72
C	Dry ash free	77.35
H	Dry ash free	5.09
O	Dry ash free	14.97
N	Dry ash free	1.51
S	Dry ash free	1.08

measurements of gas composition, gas temperatures and flow velocities. The gas composition measurement is performed simultaneously with a non-dispersive infra-red analyser (NDIR), a Fourier transform infra-red spectrometer (FTIR) and a UV-photometer. Special focus is drawn on the detection of the species affecting the NO_x formation and reduction, namely volatiles plus NO_x precursors, such as NH₃ and HCN. All of these components are measured by FTIR spectroscopy. In order to avoid condensation the whole measuring section is heated above 200 °C. The NO_x species and carbonaceous species are simultaneously measured by FTIR and NDIR to gain confidence in the outcome.

The velocity field is determined by applying Laser Doppler Velocimetry (LDV). It is performed without inserting a probe into the furnace by means of a back scattering probe and a beam expander. For each port, this probe is horizontally moved along the radial axis by a motorized bench. In this configuration, axial and tangential velocity components are measured. The grid of local measurements of flow velocities along the horizontal radial axis is chosen for each axial position to correspond to the other local measurements, such as those done for temperature and species concentrations. In the vicinity of the turbulent jets, the grid was further refined to resolve the high local gradients. LDV measurements basically require the seeding of fine particles in the flow. In the present case, this is naturally done by coal in the central coal jet and by ash particles outside the jets due to the large recirculation ratio in the furnace. The secondary air jet is however seeded with ZrO₂ particles using a fluidized bed seeding system. These particles behave almost slip-free.

Reaction zone structures are detected by applying chemiluminescence imaging which measures the intensity of UV-radiation from OH*-radicals present in the reaction zone. This intensity directly correlates with the concentration of the OH*-radicals. The radicals mainly originate from the oxidation of CH and C₂H by oxygen. OH* directly forms in an excited state (marked by an asterisk) and emits UV-radiation when de-exciting. The wavelength range of OH* chemiluminescence has been selected centred on 308 nm to avoid the thermal radiation of soot and hot walls. Thus, only radical spontaneous emission coming from reaction zones is collected. In the present optical configuration, owing to the measurement ports, the effective field of view is a circle of a diameter of about 188 mm. The optical axis of the imaging system is set perpendicularly to the vertical plane of the 3 jets. The exposure gate time is fixed at 1 ms because of low OH* emission level under FLOX conditions.

To complete the set of measurement data, total heat flux and radiative heat flux are measured respectively by a heat flux probe and an ellipsoidal radiometer. The probes are aligned with the inner furnace wall at each available port.

The results of two investigated FLOX operating conditions are presented at a thermal input of 230 kW_{th}. These differ in the type of carrier gas, one being CO₂ (referred to as FLOX_{CO₂}), the second air (FLOX_{air}); both are supplied at 50 °C. The combustion air is supplied via the two secondary air nozzles. Air staging is not applied here. In order to keep the air ratio constant at 1.15, the volumetric flow rate through the secondary air nozzles is adapted in FLOX_{CO₂}. The resulting change in velocity thereby is small and the achieved velocities stay within the intended range. The combustion air is preheated up to 150 °C.

4. Results

This experimental investigation is intended to obtain a detailed set of data. Extensive investigations of the influence of the geometrical burner parameters on FLOX combustion were already conducted by Ristic [9].

As mentioned above, the two investigated FLOX configurations differ in their type of coal carrier gas. The difference is shown in Fig. 2, which depicts the incoming coal jet at a vertical distance of 80 mm from the burner. The use of CO₂ as fuel carrier (FLOX_{CO₂}, Fig. 2a) postpones the combustion, which is evidenced by a discernible coal particle stream. In cases where air is used (FLOX_{air}, Fig. 2b), a flame structure is already observable in an early state. Nevertheless a stable attached flame does not appear.

The topology and intensity of the reaction zones are determined by OH* chemiluminescence imaging. In Figs. 3 and 4, the position of the burner is indicated by the primary nozzle along the furnace axis and the two secondary air nozzles next to it. The measured intensities are normalised with the results of a standard diffusion flame burner. In Fig. 3, the normalised images of OH* chemiluminescence are shown for the case FLOX_{CO₂} obtained from the available optical ports. The viewing direction corresponds to the normal of the jet plane, see Fig. 1b. No OH* spontaneous emission, i.e. reaction zone, is observed at the exit of the burner, confirming the initial visual impression gained from Fig. 2. The main reaction zone is found lifted far downstream between x = 450 mm and 1100 mm. The onset of the reaction zone corresponds to the region where the air jets begin to interact with the central coal jet. The highest local heat release is observed at around x = 900 mm where the entire central coal jet is entrained by the air jets (see Fig. 3). The local heat release remains low since the maximum level of OH* chemiluminescence is lower than 10% of that obtained from a flame attached to the burner exit in a standard combustion regime.

In Fig. 4, a close-up of mean normalised OH* images of the near burner region is shown for FLOX_{CO₂} on the left part and FLOX_{air} on the right part. It can be seen that the onset of reaction for FLOX_{air} located after the coal jet exit of the burner is induced by the oxygen contained in the carrier gas. Downstream the higher oxygen availability promotes combustion and high intensities are already achieved at around x = 500 mm. Moreover, the maximum combustion intensity is doubled in FLOX_{air} as compared to FLOX_{CO₂} from 7 to 15%, but it is still very small as compared to the maximum observed in a standard flame combustion regime (100%). It can be concluded that the local heat release remains very low in the lifted reaction zone, since the oxygen-lean carrier gas delays and mitigates the combustion process even further.

The LDV measurements presented in the following are obtained under FLOX_{CO₂} conditions. Due to different volumetric flow rates, the velocities vary between the two operating conditions. However, the shapes of the obtained profiles are assumed to be very similar to one another, since the geometrical patterns are not altered. In Fig. 5, three radial profiles of the axial velocity component are shown along three vertical positions in the furnace. One of the reported planes is formed by the two combustion air jets and the coal jet (jet plane), the second one is perpendicular to the first one and referred to as recirculation plane.

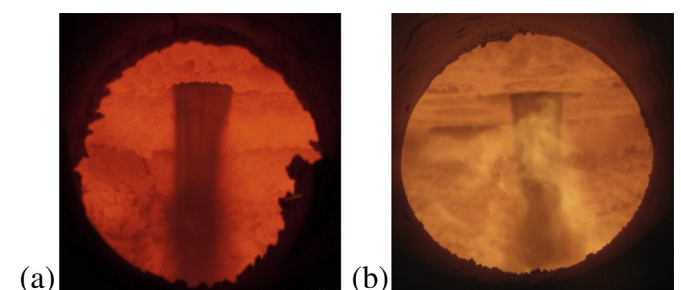


Fig. 2. Photographs at the exit of the burner (a) FLOX_{CO₂} (b) FLOX_{air}.

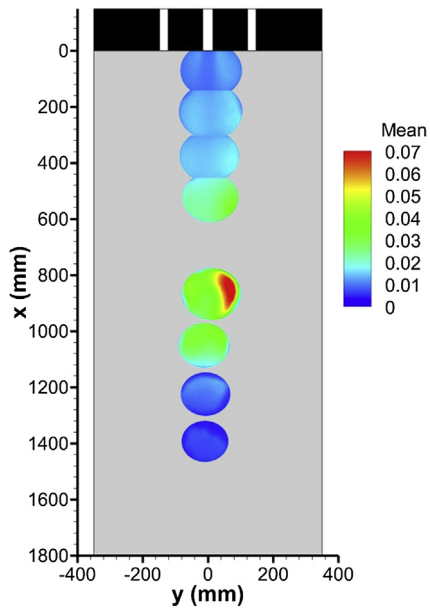


Fig. 3. Mean normalised images of OH^* chemiluminescence for $\text{FLOX}_{\text{CO}_2}$.

The profile closest to the burner at $x = 230$ mm reports the high velocities and thus the highest momentum of combustion air jet. A minor velocity maximum is found along the furnace axis induced by the incoming coal jet. In the recirculation plane, the recirculation zone is identified by negative velocity values. It is also observed that only a slight recirculation occurs within the jets plane due to the spatial restrictions imposed by the furnace. Further downstream at $x = 1060$ mm, the maximum velocity along the furnace axis vanishes and the combustion air velocity is reduced by 66%. One can observe that the recirculation velocity within the recirculation plane reaches its maximum at around -11 m s^{-1} and the recirculation zone spreads from the combustion air jet position towards the furnace wall. After 1890 mm from the burner exit, little

recirculation still occurs along the recirculation plane in the furnace wall vicinity whereas the jets plane demonstrates a uniform plug flow.

The gas concentrations obtained for the nitrogenous species NO_x , NH_3 and HCN are presented in Fig. 6. At $x = 230$ mm one can see that the furnace is divided by the combustion air jets into a high-level NO_x region around the furnace axis ($0 \text{ mm} < y < 100 \text{ mm}$) and a recirculation region ($200 \text{ mm} < y < 350 \text{ mm}$), characterized by a lower and uniformly distributed NO_x level. The NO_x precursors NH_3 and HCN are only present around the coal jet in the burner vicinity. When they mix with the incoming combustion air at around $y = 150$ mm, these become immediately oxidised. Furthermore, the difference between released HCN and NH_3 is noteworthy. In FLOX_{air} where higher temperature and oxygen levels are achieved, the release of HCN from the coal jet is promoted. In $\text{FLOX}_{\text{CO}_2}$ on the other hand, the amount of NH_3 released is doubled, but the amount of HCN amount is about 90% lower than that obtained with FLOX_{air} .

Regarding the temperature levels (see Fig. 7) in $\text{FLOX}_{\text{CO}_2}$ and FLOX_{air} , the difference lies at a maximum of about 100 K. Then, the significant difference in NO_x values reported in Fig. 6 can be explained by a change in the oxygen availability. Fig. 7 highlights the lack of oxygen around the furnace axis for $\text{FLOX}_{\text{CO}_2}$, resulting in NO_x formation lowered by 25%. It is stated that the temperatures measured at $x = 230$ mm and 1230 mm are uniform and of the same magnitude for both $\text{FLOX}_{\text{CO}_2}$ and FLOX_{air} across the furnace diameter; only the region on the incoming combustion air jets differs. This indicates a good recirculation and mixing, thus confirming the characteristic homogeneous temperature profile known for a FLOX regime. Further downstream the different profiles are homogeneous with constant spreads in temperature and NO_x and O_2 concentrations.

Comparing the NO_x concentrations (Fig. 6) measured in the recirculation zone at $x = 230$ mm and across the whole furnace diameter at $x = 1230$ mm, a reduction of about $100 \text{ mg/m}^3_{\text{stp}}$ is observable at $x = 230$ mm for both FLOX cases. At the same location, the low oxygen concentration (Fig. 7) indicates a reducing atmosphere which promotes NO_x -reduction in the recirculating flue gas.

Table 2 compares the emissions measured at the furnace exit. It can be seen that the oxygen concentrations are similar.

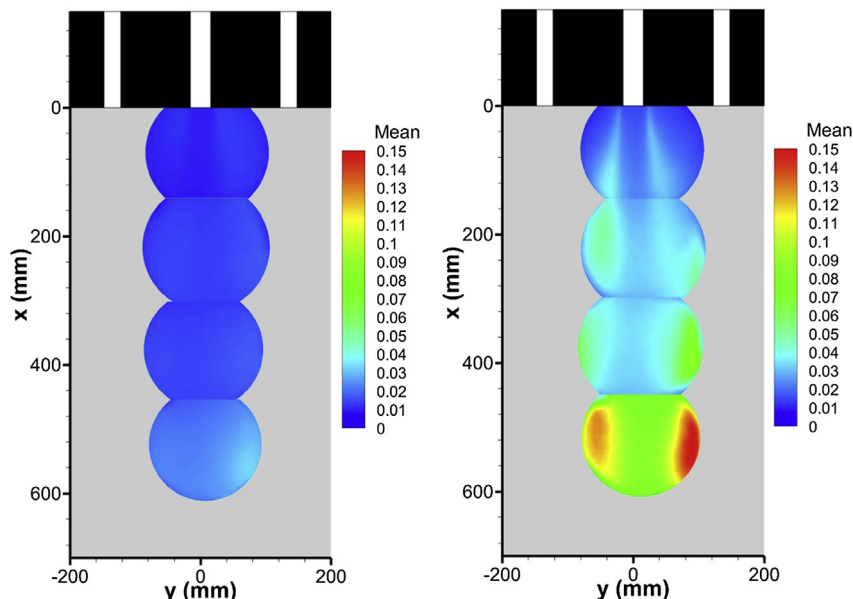


Fig. 4. Mean normalised OH^* intensities for $\text{FLOX}_{\text{CO}_2}$ (left) and FLOX_{air} (right).

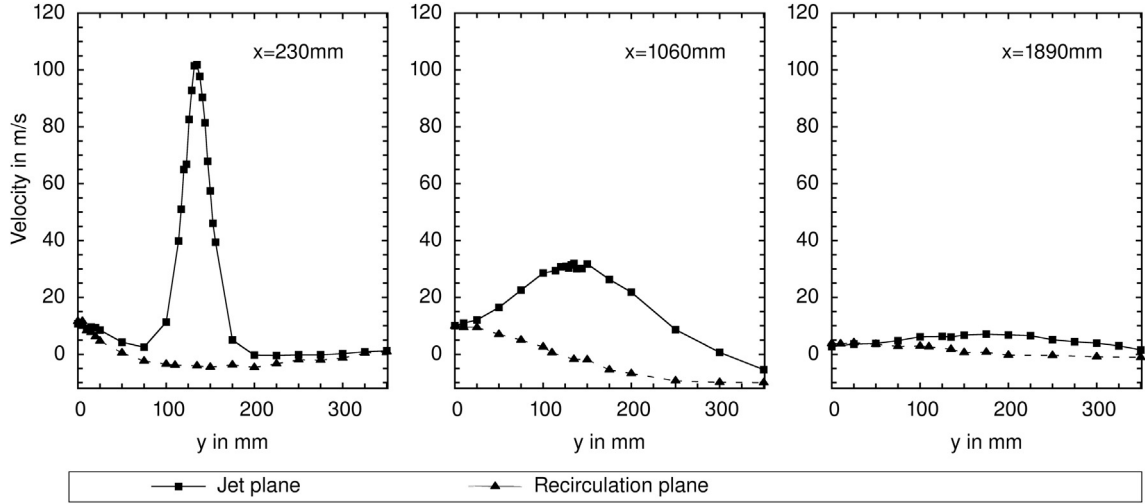


Fig. 5. Radial profiles of axial velocity in the jet and recirculation plane.

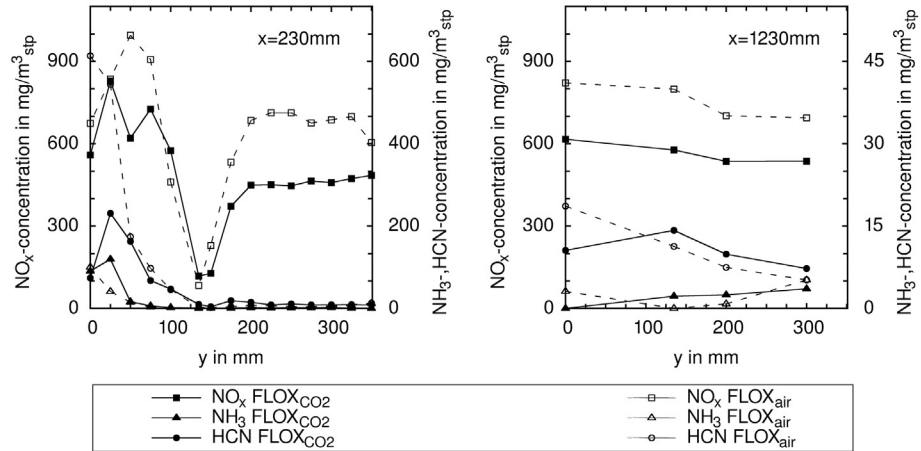


Fig. 6. Radial profiles of NO_x -, HCN - and NH_3 -concentrations (dry) in the jet plane.

Unsurprisingly, the CO and NO_x concentrations differ: as mentioned above, the lack of oxygen in $\text{FLOX}_{\text{CO}_2}$ results in lowered NO_x emissions along with increased CO emissions. This behaviour is similar to that one obtained with air staging of flame burners.

The measured heat flux profiles are as homogeneous as the temperature profiles over the whole furnace length. The maxima are found to correspond with those of OH^* emission. Comparing $\text{FLOX}_{\text{CO}_2}$ to a standard flame burner in terms of heat flux, the maximum is about one third lower.

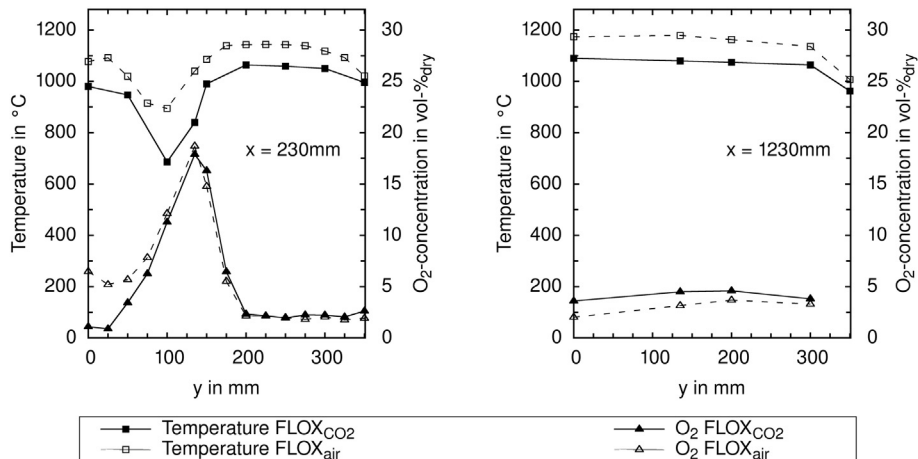


Fig. 7. Radial profiles of gas temperature and O_2 -concentration (dry) in the jet plane.

Table 2
Furnace exit emissions (dry).

		FLOX _{CO₂}	FLOX _{air}
O ₂	vol-%	2.8	2.9
CO	mg/m ³ _{stp} @ 6 vol-% O ₂	188	50
NO _x	mg/m ³ _{stp} @ 6 vol-% O ₂	391	611

5. Conclusions

Within the experimental campaign reported here for flameless oxidation of pulverized coal, the reaction zone topology and the dominating flow patterns have been identified by means of OH* chemiluminescence and LDV. Both techniques illustrate the principle features of FLOX combustion, i.e. high recirculation flow rates, low reaction intensity and wide spread volumetric reaction zones. It is also demonstrated that the absence of oxygen within the carrier gas alters the pyrolysis, delays the oxidation and reduces the NO_x formation. This fact should be kept in mind when further optimizing the FLOX concept for pulverized coal combustion: dilution of the carrier gas is more cost-effective than dilution of the combustion air. Nitric oxides and their precursors are identified in combination with other gas species, such as O₂, CO and volatiles. Furthermore, the gas temperatures are mapped and offer important information about the temperature distribution and the effects on the NO_x formation and consumption: lower temperatures together with fuel-rich conditions reduce the HCN release and NO_x formation. Finally, the heat flux profile obtained affirms the homogeneity of this combustion technology. To further lower the NO_x emissions from pulverized coal flames, air staging is an additional measure which has already shown its potential in the investigations of Ristic [9].

For a better understanding of the complex formation and reduction paths occurring during FLOX combustion, the acquired

data will be used within CFD-simulations in a next step. An adapted NO_x sub-model governing the considerably most important NO_x formation and reduction equations will be applied. Thereby the door is pushed open for further optimization of the burner geometry and the flameless oxidation process for pulverized coal combustion.

Acknowledgements

The authors gratefully acknowledge the financial support from the European Commission which supported this project within the Research Fund for Coal and Steel (Project number RFCR-CT-2011-00005).

References

- [1] J.A. Wünnig, J.G. Wünnig, Flameless oxidation to reduce thermal NO-formation, *Prog. Energy Combust. Sci.* 23 (1997) 81–94.
- [2] M. Katsuki, T. Hasegawa, The science and technology of combustion in highly preheated air, *Proc. Combust. Inst.* 27 (1998) 3135–3146.
- [3] S. Orsino, M. Tamura, P. Stabat, S. Constantini, O. Prado, R. Weber, Excess Enthalpy Combustion of Coal, IFRF Doc. No. F46/y/3, 2000.
- [4] A. Cavalieri, M. de Joanon, Mild combustion, *Prog. Energy Combust. Sci.* 30 (2004) 329–366.
- [5] C.P. Fenimore, Formation of nitric oxide in premixed hydrocarbon flames, in: *Symp. (Int.) Comb.*, vol.13, 1971. *Comb. Inst.*, 373–380.
- [6] J. Zeldovich, The oxidation of nitrogen in combustion and explosions, *Acta Physiochim. URSS* 21 (1946) 577–628.
- [7] A.N. Hayhurst, I.M. Vince, Nitric oxide formation from N₂ in flames: the importance of “prompt” NO, *Prog. Energy Combust. Sci.* 6 (1980) 35–51.
- [8] C.P. Fenimore, H.A. Fraenkel, Formation and interconversion of fixed-nitrogen species in laminar diffusion flames, in: *Symp. (Int.) Comb.*, vol.18, 1981. *Comb. Inst.*, 143–149.
- [9] D. Ristic, Feasibility and NO_x Reduction Potential of Flameless Oxidation in Pulverised Coal Combustion (PhD Thesis), University of Stuttgart, 2012.
- [10] P.R. Solomon, M.B. Colket, Evolution of fuel nitrogen in coal devolatilization, *Fuel* 57 (12) (1978) 749–755.